26th IAEA Fusion Energy Conference
Kyoto International Conference Center, Kyoto, Japan, 17-22 Oct. 2016

Overview of Spherical Tokamak Research in Japan

Y. Takase[1], A. Ejiri[1], T. Fujita[2], N. Fukumoto[3], K. Hanada[4], H. Idei[4], M. Nagata[3], Y. Ono[1], H. Tanaka[5], A. Fukuyama[5], R. Horiuchi[6], S. Tsuji-Iio[7], Y. Kamada[8], Y. Nagayama[6], Y. Takeiri[6]
[1]U. Tokyo, [2]Nagoya U., [3]U. Hyogo, [4]Kyushu U., [5]Kyoto U., [6]NIFS, [7]Tokyo Inst. Tech., [8]QST, Japan

Nationally Coordinated Research Using Various ST Devices*

*TST-2, TS-3, TS-4, UTST, TOKASTAR-2, LATE, HIST, QUEST + theory/modeling

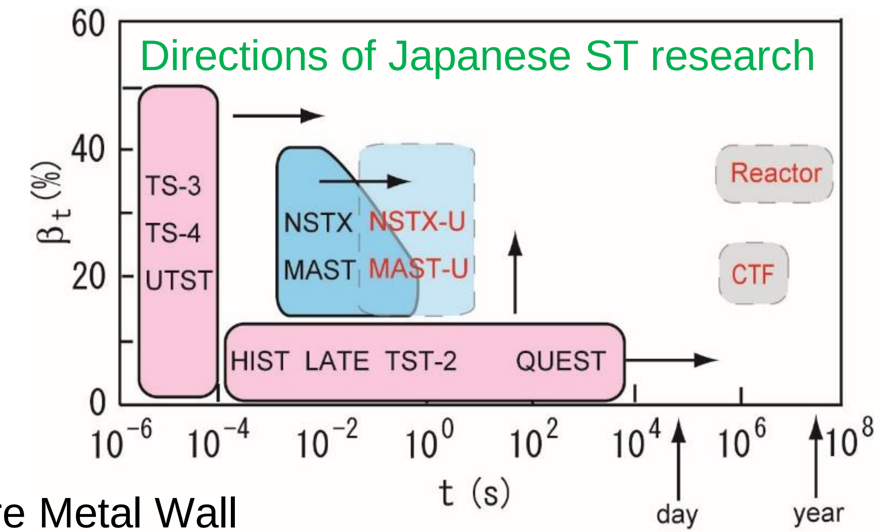

Contents

- I_p Start-up
  - RF Waves: ECW/EBW, LHW
  - CHI
  - AC OH
- Advanced Fueling
  - CT Injection
- Steady-State Operation
  - Particle Control by High Temperature Metal Wall
- Ultra-High-β Operation
  - Reconnection Heating by Plasma Merging
- Low-A Tokamak-Helical Hybrid
  - Stability Improvement by Helical Field

Non-inductive Production of Extremely Overdense ST Plasma by EBW Excited via O-X-B Method in LATE

Extremely overdense ST plasmas are produced non-inductively with EBW excited by O-X-B mode conversion when EBW is excited in the 1st propagation band (between ω_{ce} and $2\omega_{ce}$ layers). Density reaches ~ 6 times the cutoff density for 5 GHz microwave.

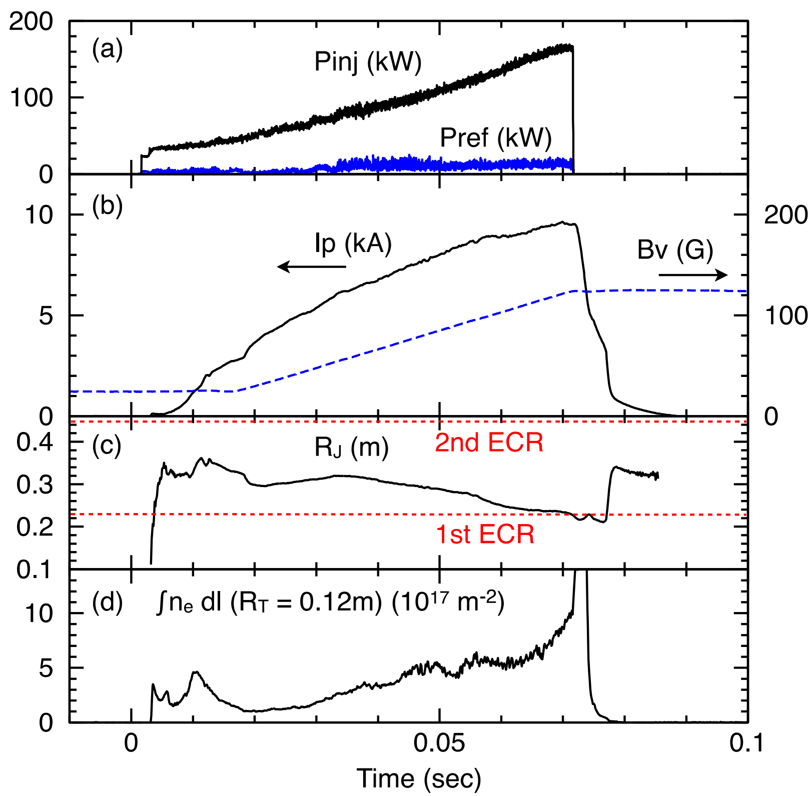

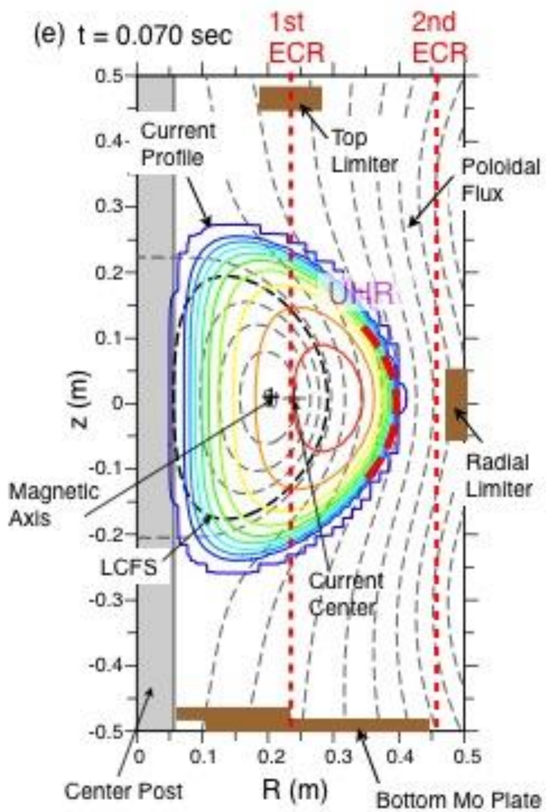

Density and soft X-ray emission increases when the $2\omega_{ce}$ layer is located on the outboard side of the upper hybrid resonance (UHR) layer, i.e., when EBW is excited in the 1st propagation band. Such B_t dependence is observed at two different microwave frequencies.

5GHz Microwave

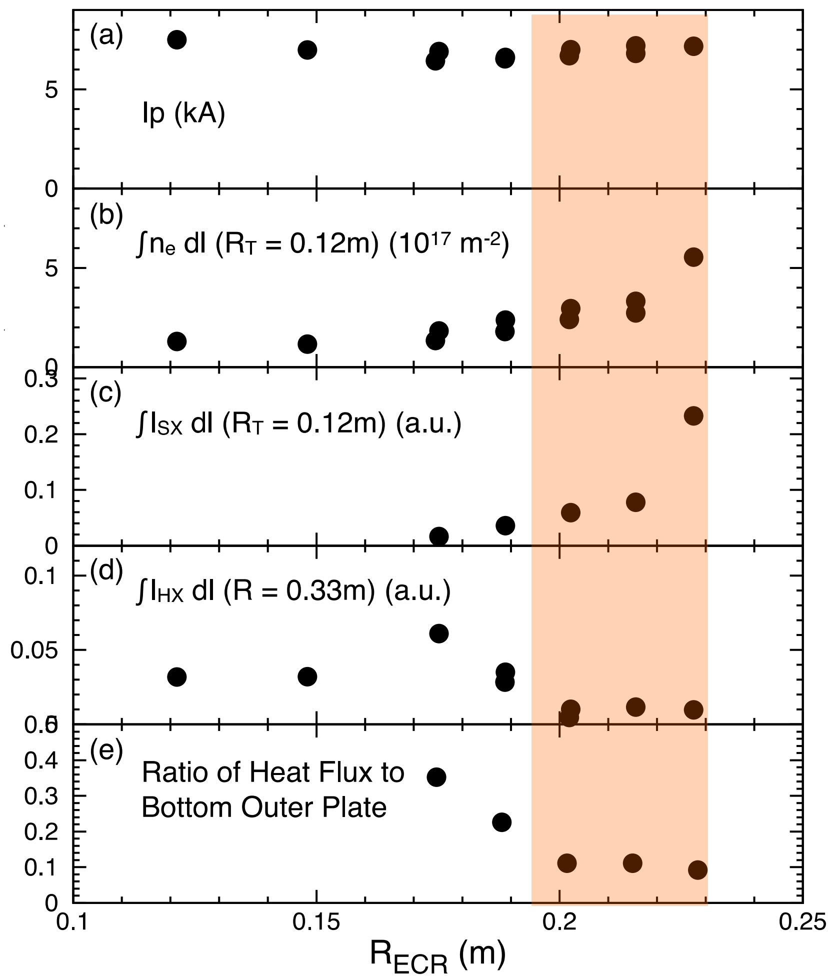

2.45GHz Microwave

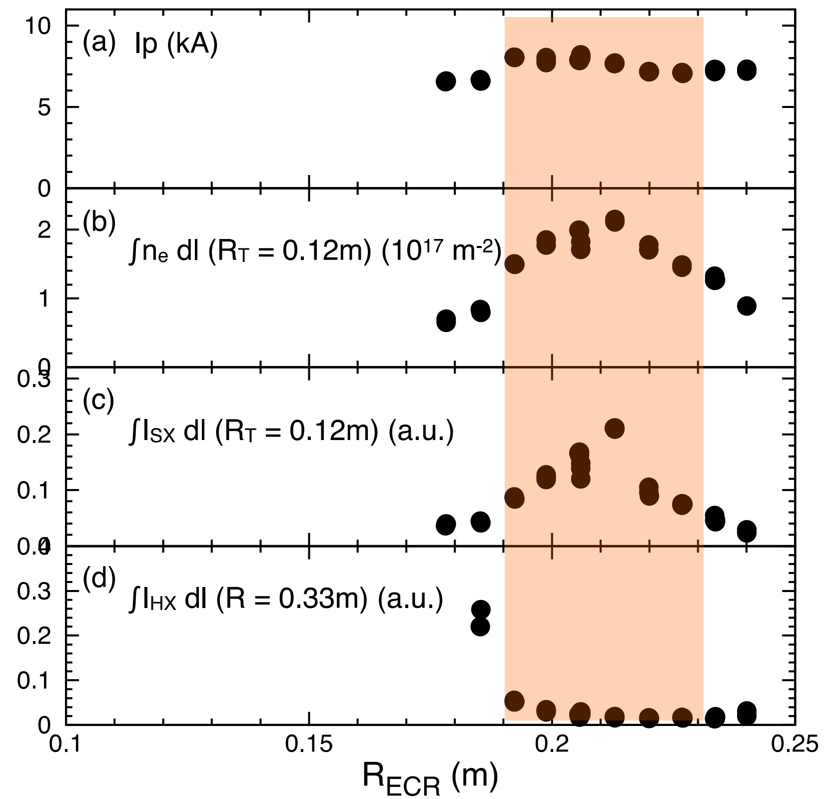

Fukuyama, et al.

1-D Kinetic Full-Wave Analysis of O-X-B Mode Conversion by TASK/W1

Integral-operator form of dielectric tensor to describe finite Larmor radius effects

Parameters of LATE
B = 0.08 T, n_{e0} = 10^{17} m^{-3}

Antenna loading resistance vs $k_{//}$

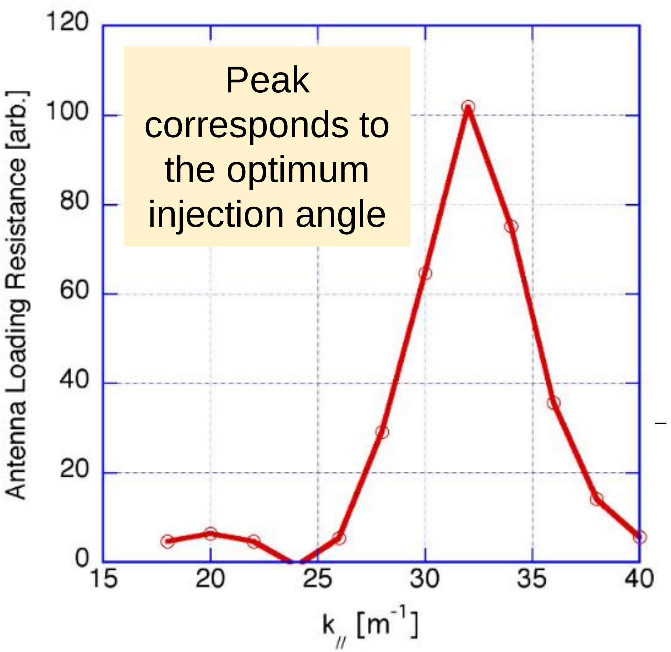

Perpendicular wave number vs. major radius

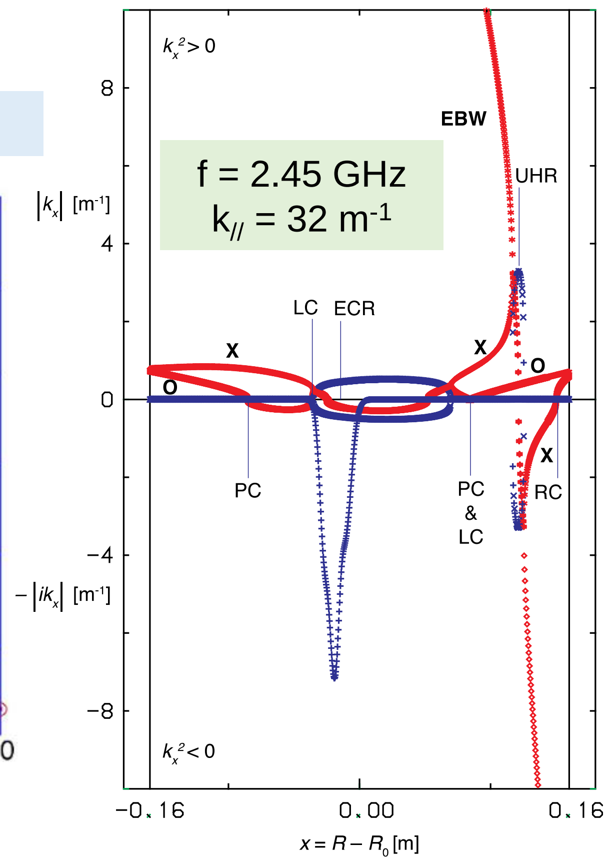

Wave structure vs. major radius

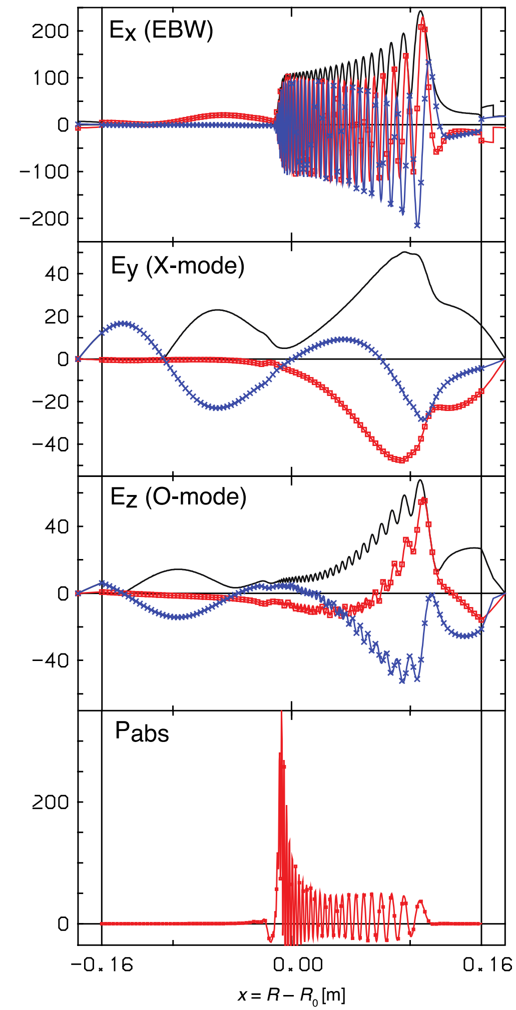

Non-inductive ECH/CD with Waves at Two Frequencies (8.2 GHz / 28 GHz) in QUEST

EX/P4-50 H. Idei, et al.

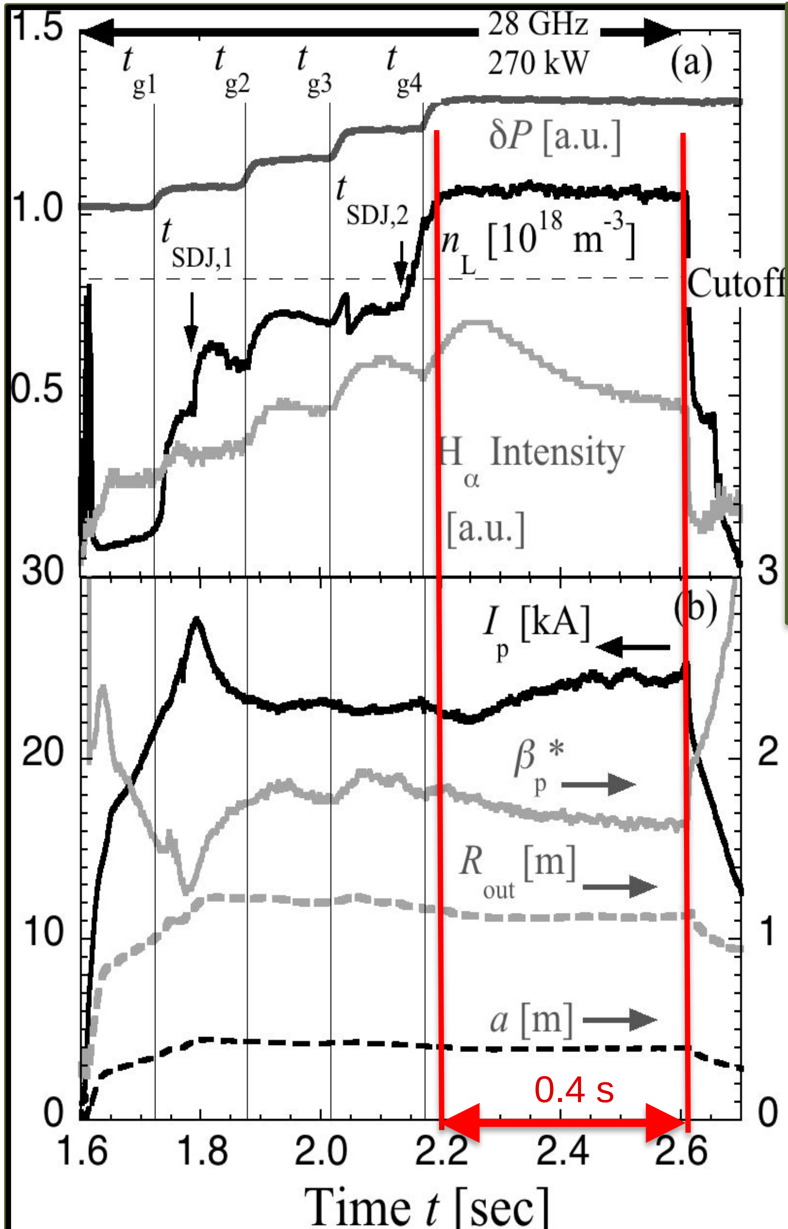

Microwave power was injected at two frequencies (8.2 GHz and 28 GHz) simultaneously for fully non-inductive I_p start-up and sustainment in QUEST.

Gas puff timings are indicated with δP increments ($t = t_{g1}$, t_{g2}, t_{g3} and t_{g4}).

H_α intensity increased at gas puff timings. Density sometimes increased spontaneously without gas puff.

Spontaneous density jumps (SDJs) were observed twice ($t = t_{SDJ1}$ and t_{SDJ2}) in this discharge, and the density exceeded the cutoff density for 8.2 GHz.

Equilibrium electron pressure profile was bell-shaped.

Flux surfaces are densely spaced on the low-field side.

Overdense 25 kA plasma with central high energy electron pressure was built up non-inductively and sustained for 0.4 s.

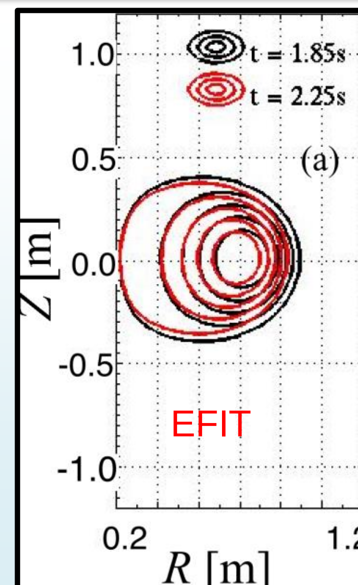

High bulk T_e was observed near $2\omega_{ce}$ layer for 28 GHz, while a local T_e peak was observed near ω_{ce} layer for 8.2 GHz only before the 1st SDJ at t=1.75 s.

Measured bulk pressure P_e profile was hollow, resulting from the off-axis heating at the $2\omega_{ce}$ layer and radiation cooling after SDJs.

Current density profile and equilibrium pressure profile (EFIT) are centrally peaked.

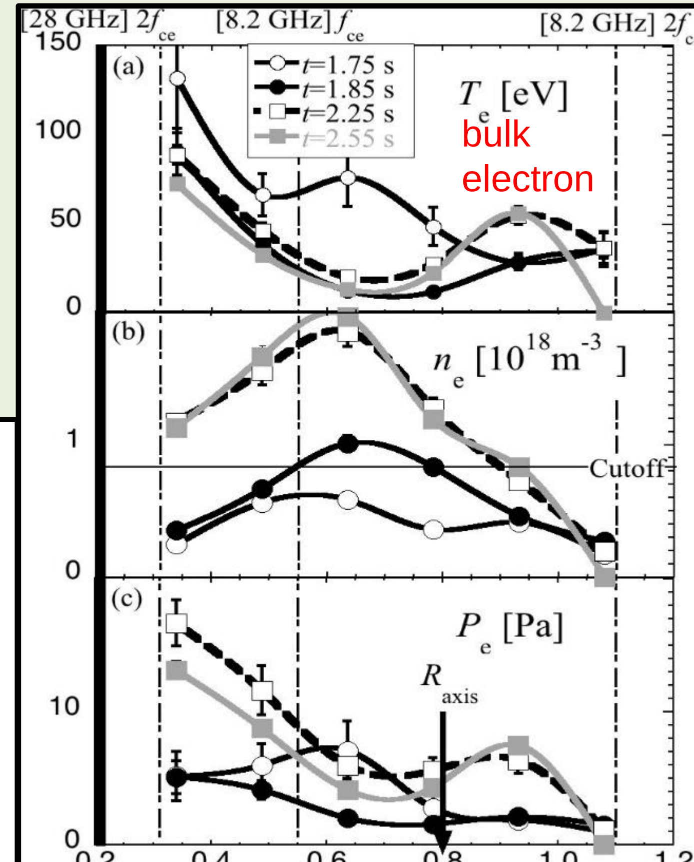

Hard X-ray emission at high energies (>200 keV) was observed from the central overdense region, while bulk P_e was larger on the high-field side off-axis region near the $2\omega_{ce}$ layer for 28 GHz.

There were abundant energetic electrons in the central overdense region.

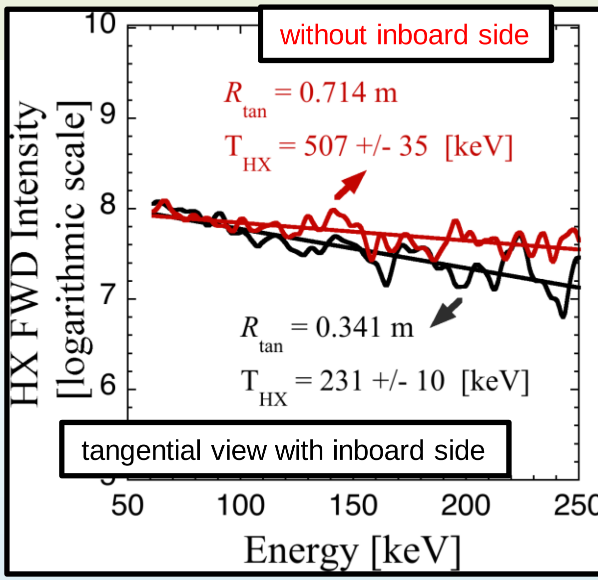

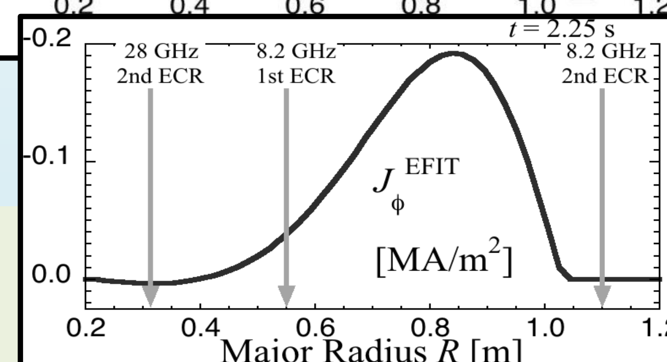

Bulk T_e and P_e increased in the overdense region where there are Doppler-shifted ω_{ce} resonance layers for large $N_{//}$.

Local ECH/CD Non-inductive I_p Start-up in QUEST

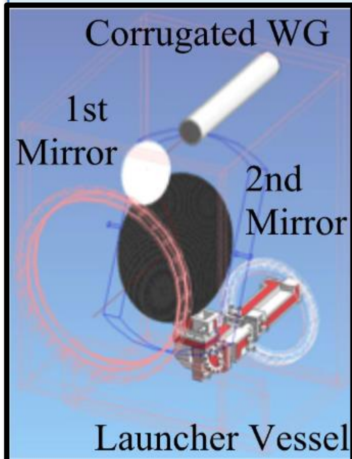

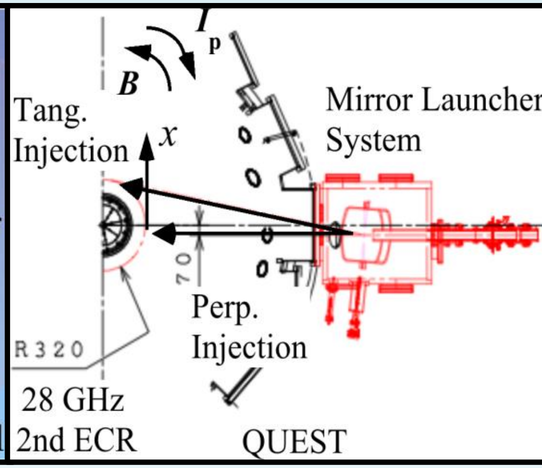

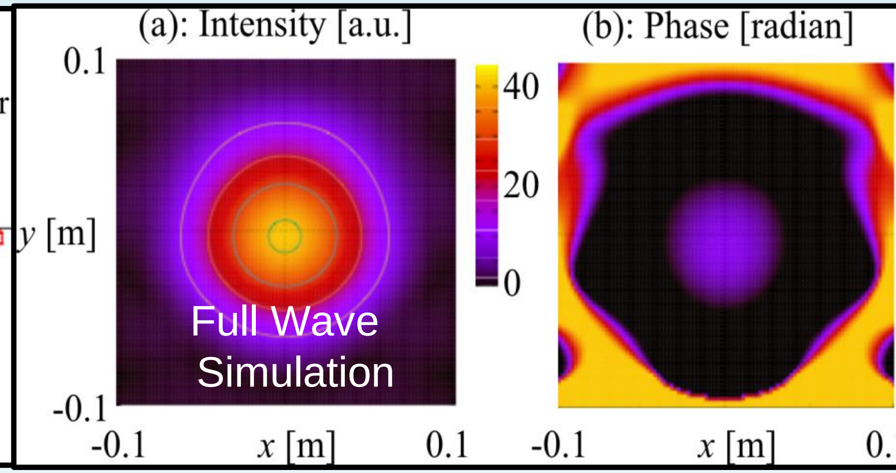

Kirchhoff integral code was used for mirror design.
Mirror performance at 28 GHz was checked by 3-D full-wave simulation.
Sharply focused beam with small beam size (0.052 m) was obtained.
The 2nd focusing mirror can steer the beam in the toroidal direction.

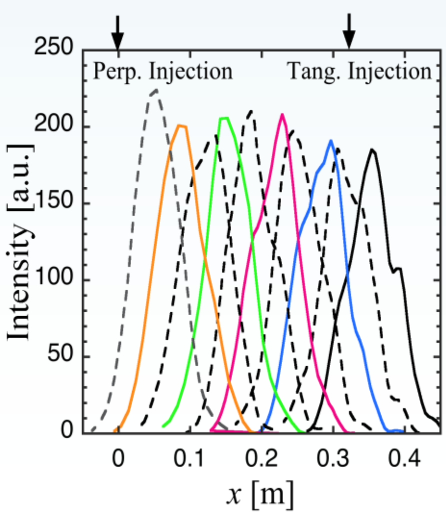

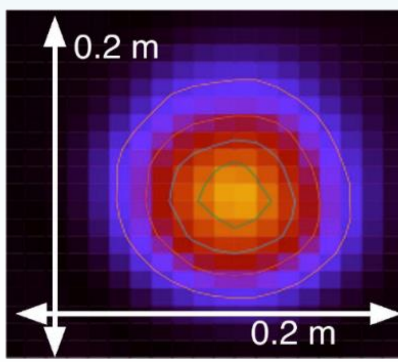

Focused beam measured at low power

Polarization control for 2^{nd} ECH/CD

Non-inductive I_p of 70 kA was achieved using the new launcher.

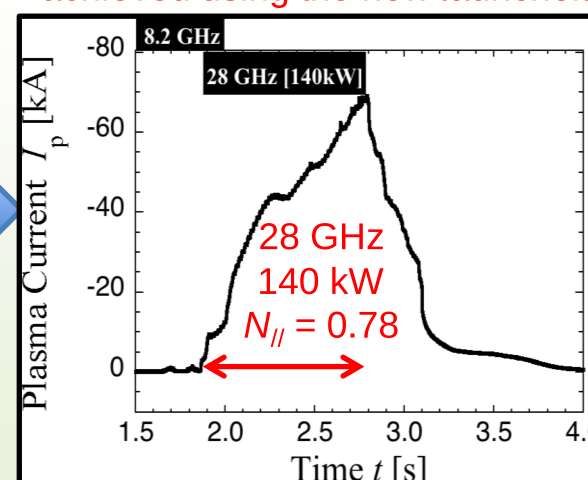

CS-less I_p Start-up by LHW

Two capacitively-coupled combline (CCC) antennas

- Traveling LHW is excited directly
- Sharp $n_{||}$ spectrum & high directivity

Outboard-launch

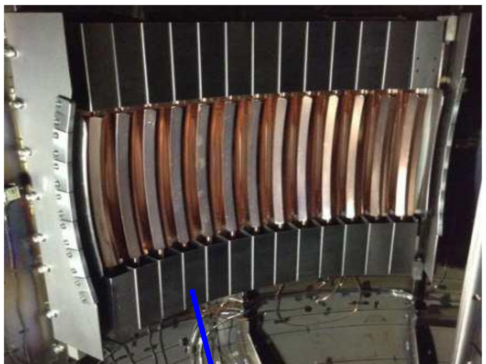

Top-launch

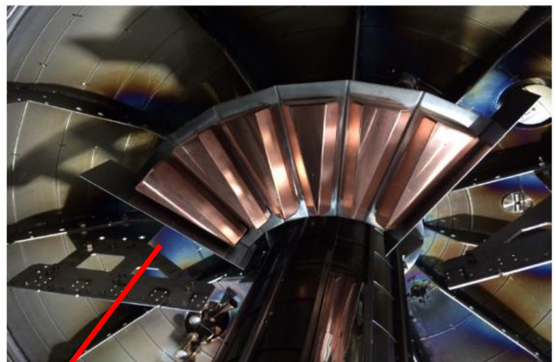

(installed in March 2016)

TST-2

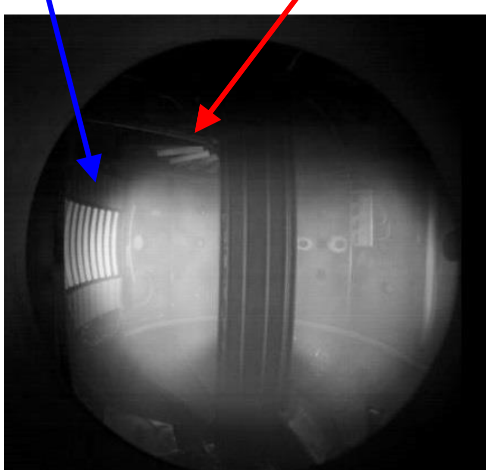

Good core accessibility and deposition are expected even at high n_e.

I_p = 25 kA achieved with outboard-launch antenna alone (improved from 16 kA)

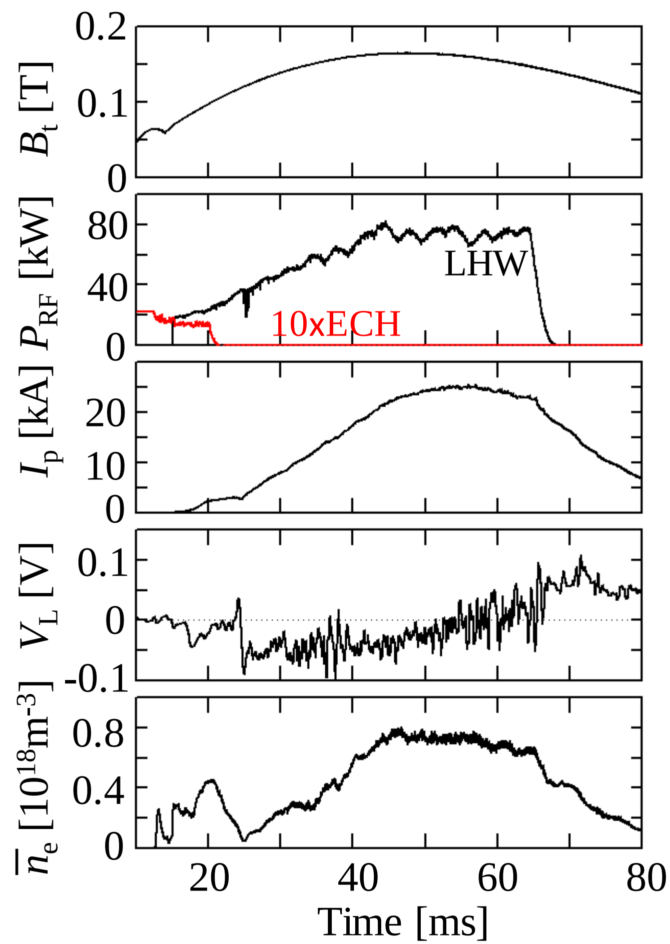

collaboration with Moeller (GA, US)

Sustained I_p increases with n_e and B_t

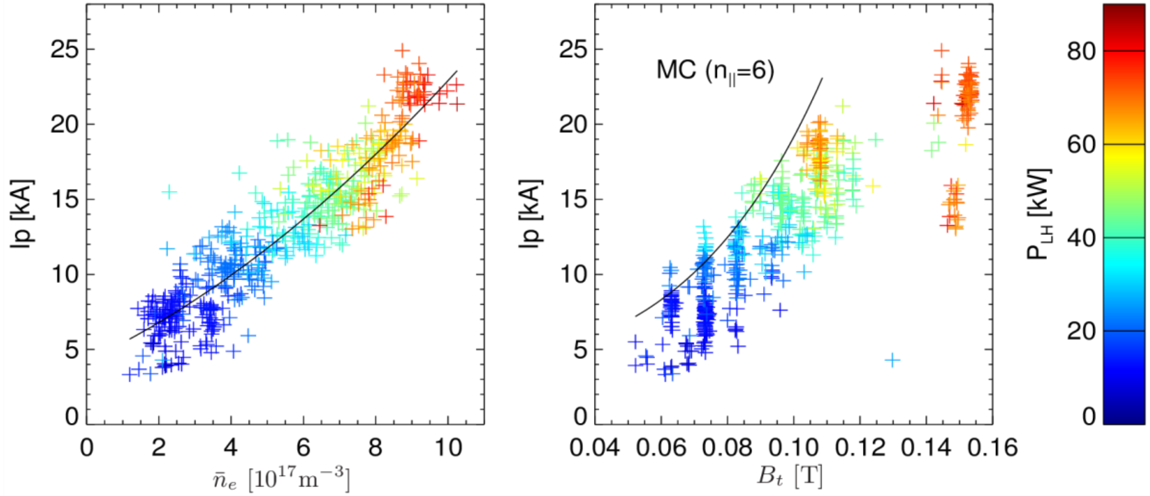

Comparison of discharges sustained by outboard-launch and top-launch antennas

I_p of up to 13 kA is sustained by the top-launch antenna alone. However, precise plasma position and size control during the initial I_p ramp-up phase is difficult.

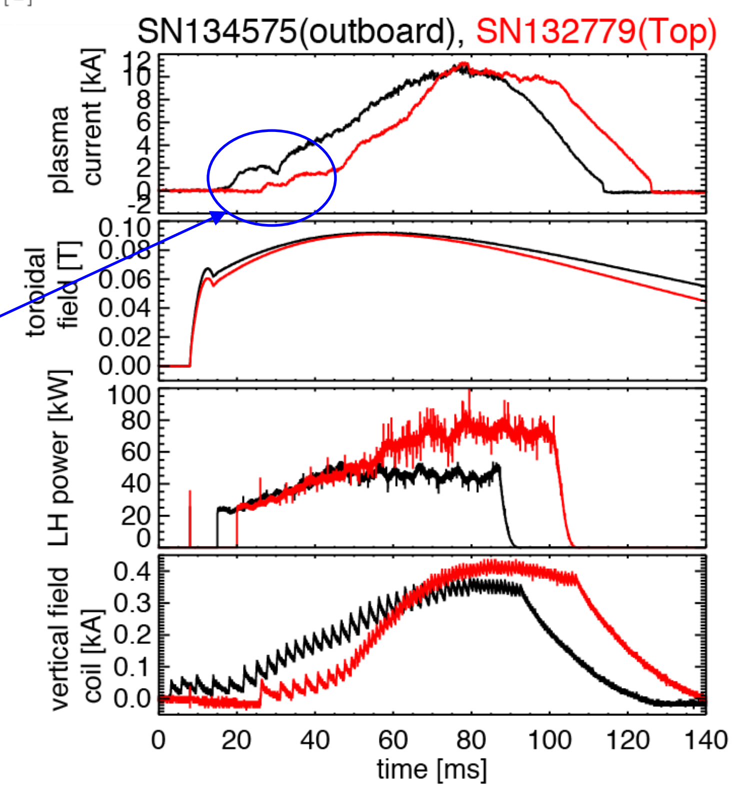

➡ Use outboard-launch for start-up and top-launch for ramp-up.
(initial experiment in progress)

Coaxial Helicity Injection (CHI)

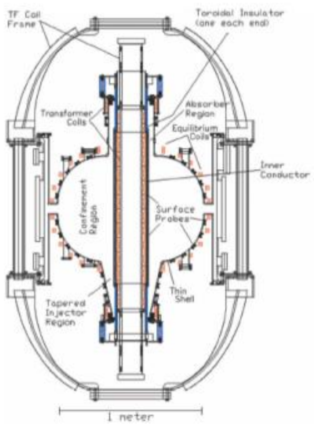

HIT-II
(U. Washington)

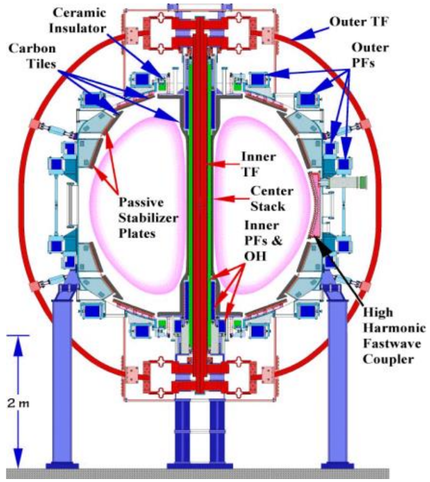

NSTX
(PPPL)

HIST
(U. Hyogo)

QUEST
(Kyushu U.)

- These ST devices in US and Japan aim to develop and understand non-inductive CHI start-up/ramp-up that is necessary for the viability of ST reactors.
- The successful current generation up to 0.3 MA in NSTX (PPPL) validated the capability of CHI for start-up followed by inductive ramp-up to 1 MA.
- A new CHI start-up experiment with an alternate electrode and insulator con-figuration, combined with ECH, will start on QUEST (Kyushu U.) under US-Japan collaboration.
- Primary purpose of CHI experiments on HIST (U. Hyogo) is to examine the physics of flux closure and current profiles which still remain key issues of CHI.

Characteristics of ST Plasmas Generated by CHI on HIST

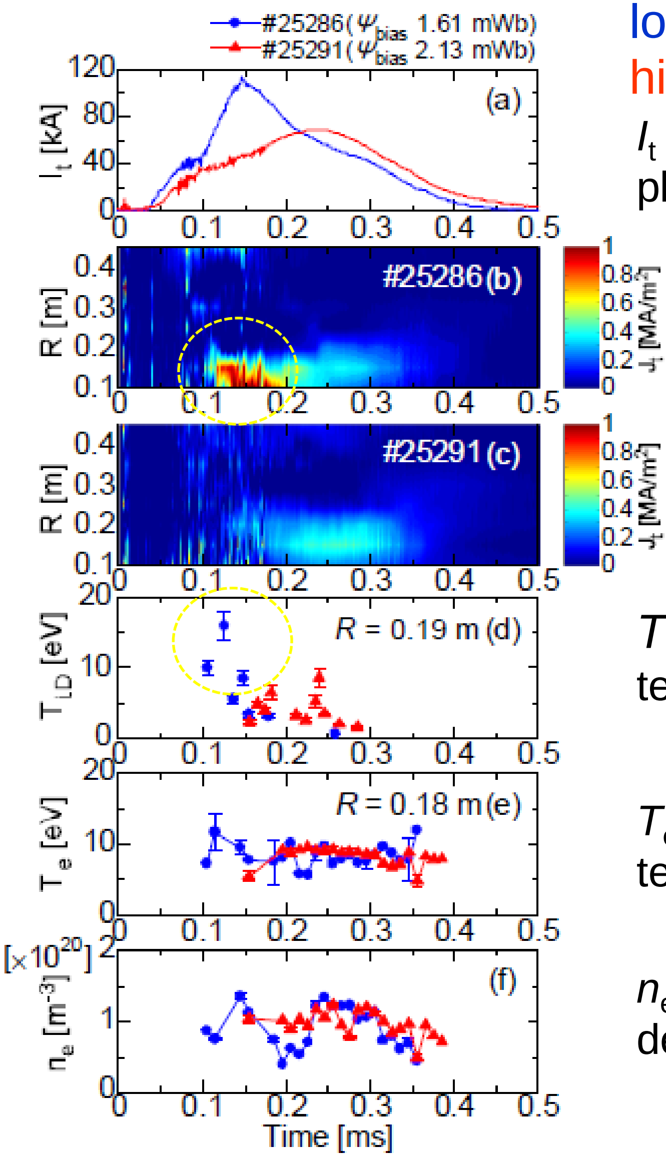

low bias flux

high bias flux

I_t : toroidal plasma current

low bias flux

$j_t(R)$: toroidal current density

high bias flux

$T_{i.D}$: Doppler ion temperature

T_e : electron temperature

n_e : electron density

Comparison of CHI generated plasmas between high and low bias flux operations.

- Peak I_p of 80-120 kA was generated by CHI. A stable closed flux formation was achieved in the high bias case.
- In the low bias case, the toroidal current density is concentrated on the inboard side, leading to kink instabilities at a later time.
- $T_{i.D}$ during the I_p rise phase in the low bias case is higher than T_e ~ 10 eV, indicating ion heating.
- n_e was ~1×10^{20} m^{-3}.

Plasmoid Formation and Flux Closure in CHI Plasmas

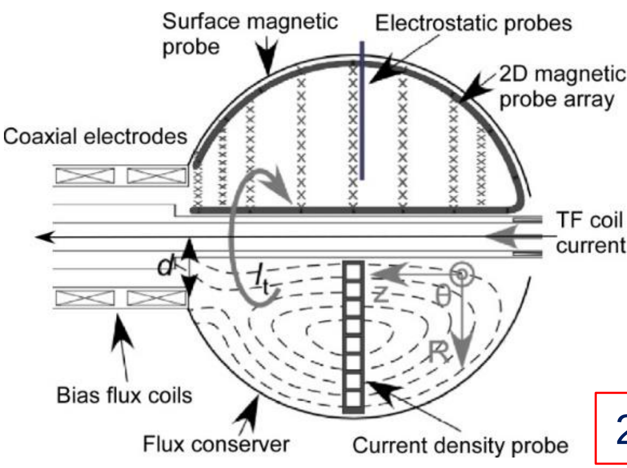

HIST

2-D contour plots

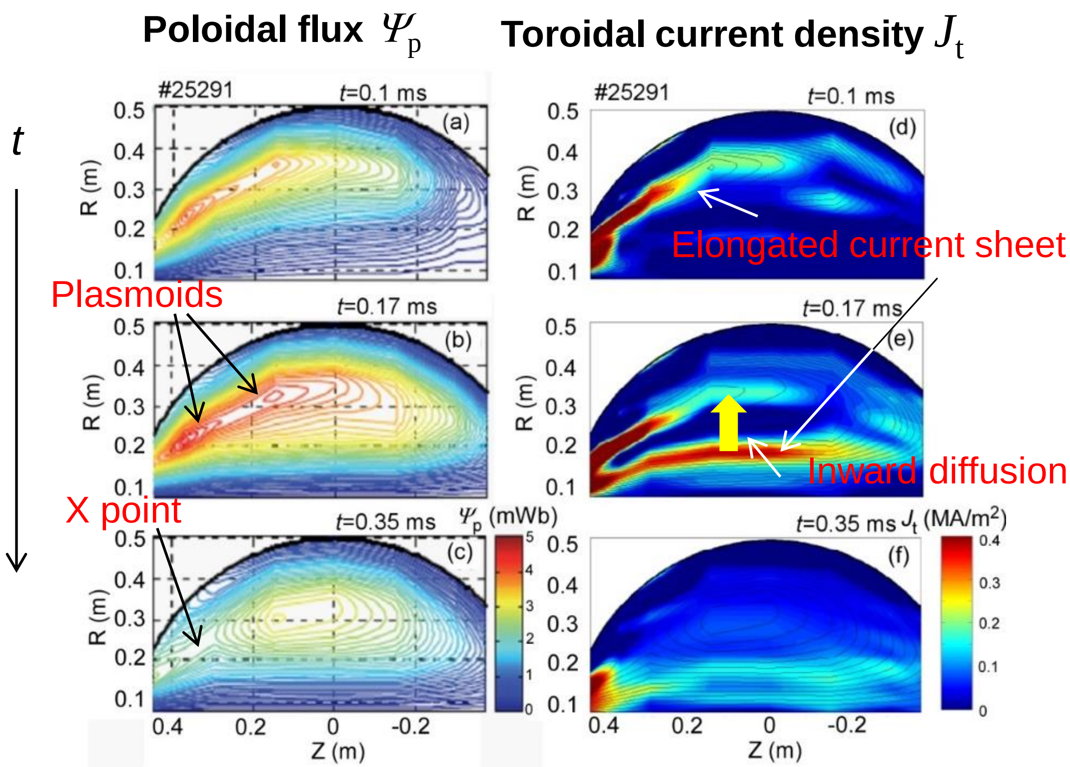

Experimental results from internal magnetic probe measurements

1. Formation of closed flux surfaces (c) was vefified. The ratio of the closed flux to the total flux is 25-30%.
2. Small-scale plasmoids (a), (b) are generated in the elongated toroidal current sheet (d), (e) in the presence of a strong B_t.
3. The plasmoid grows in size due to inward diffusion (e), (f) of the toroidal current in the open flux region during the decay phase .

AC Ohmic Heating Experiments on TST-2 (for pre-ionization and DC current drive)

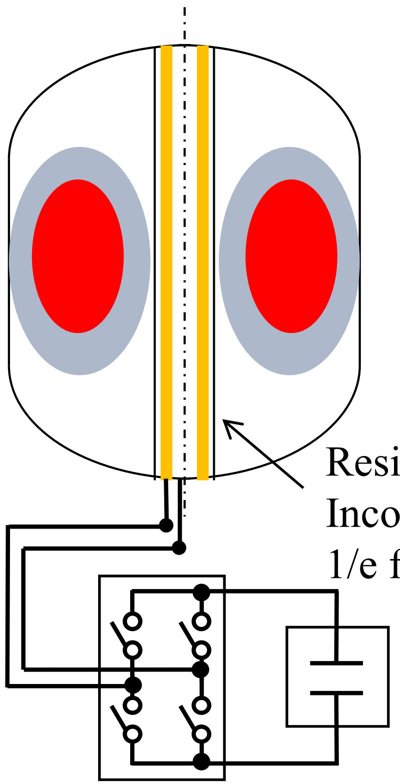

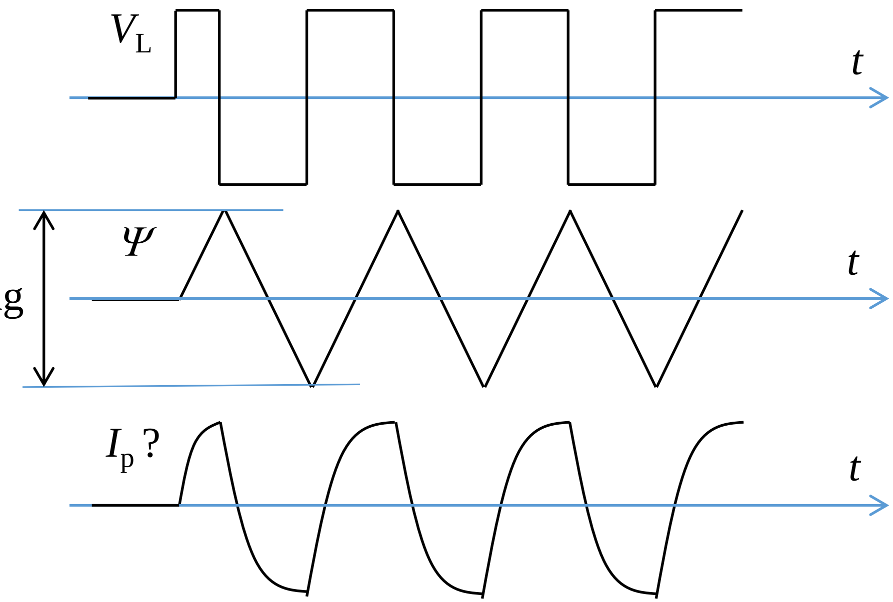

- Cumulative effect to increase n_e (pre-ionization)?
- Heating power: $<\tilde{I}_p \tilde{V}_L>$ $\rightarrow$ DC current drive?

Pre-ionization

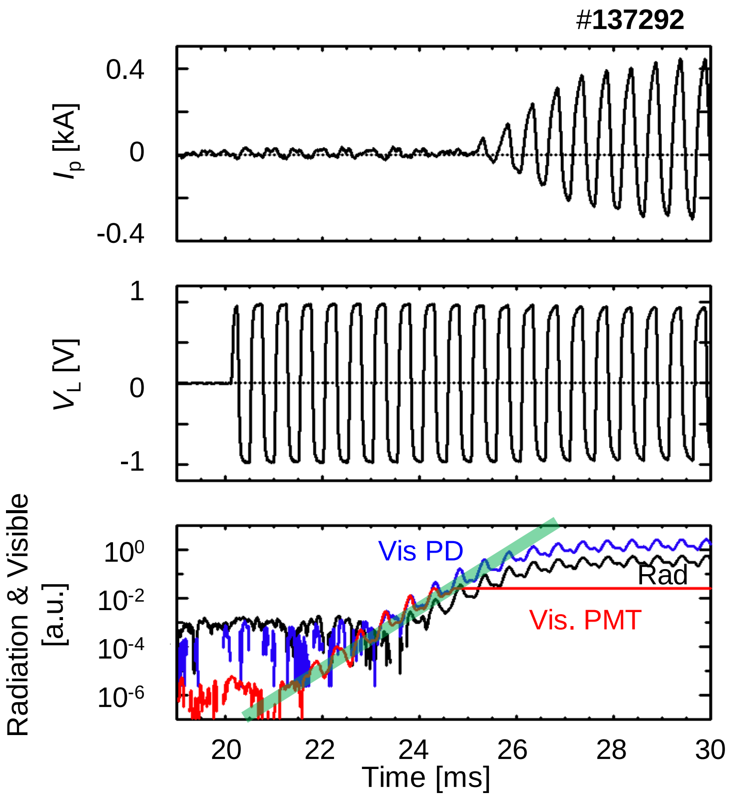

Exponential growth in emission and I_p

- The growth rate and saturation in I_p n_e can be explained qualitatively by a model based on Townsend's α.
- Successful pre-ionization with $|V_{loop}| \geq 0.5$ V (~0.6 V/m).

DC current drive

DC I_p component (<1.9 kA) appears when B_Z is applied

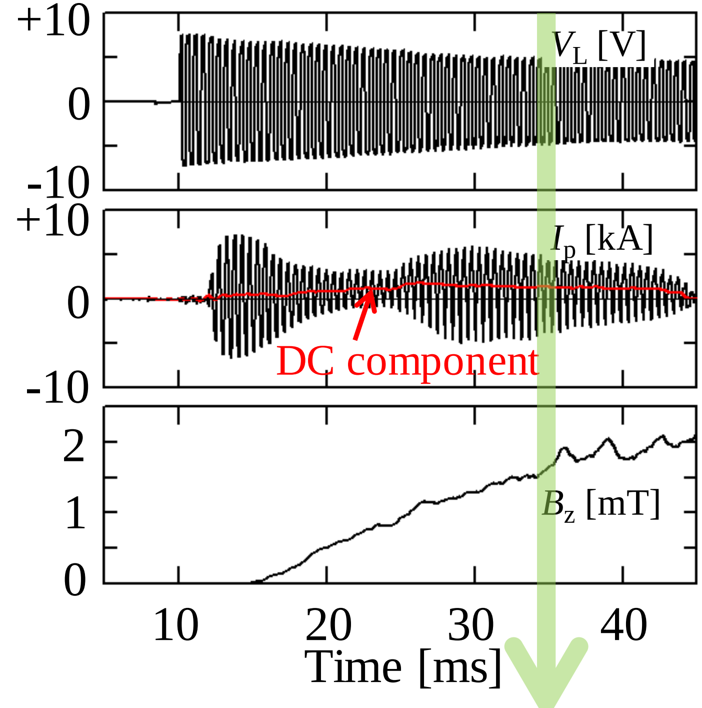

Time averaged visible camera image shows an ST configuration.

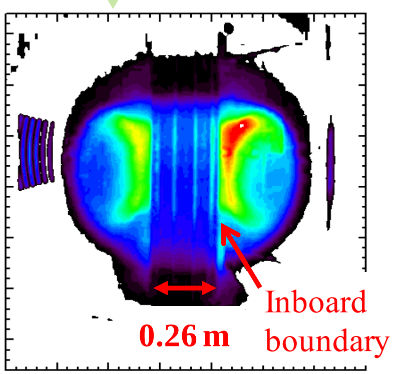

CT Injection (CTI) as Advanced Fueling on QUEST

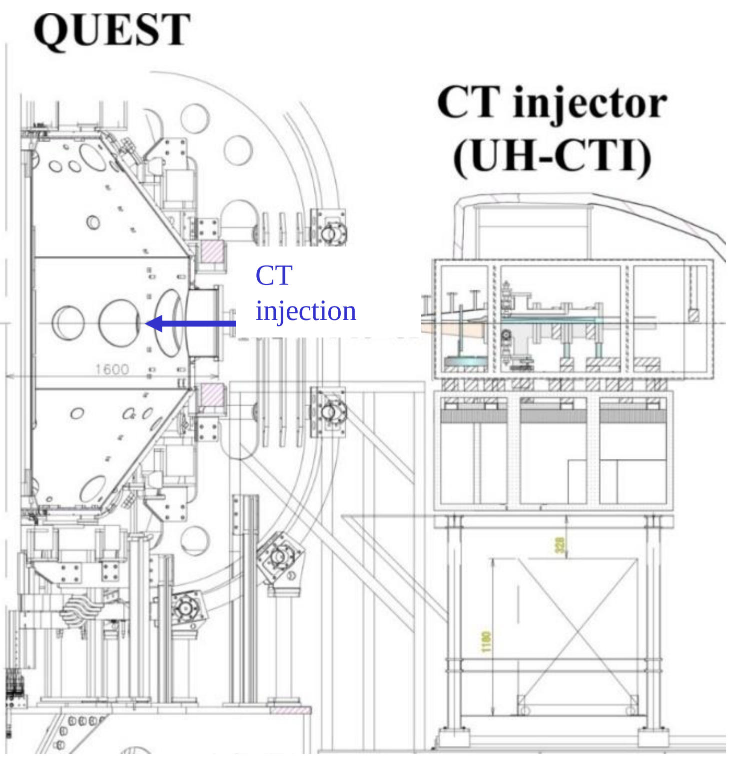

Compact toroid (CT) injection experiments have been conducted to develop an advanced fueling method.

UH-CT injector used in this experiment is capable of injecting a CT plasma that can penetrate to B_t = 0.8 T.

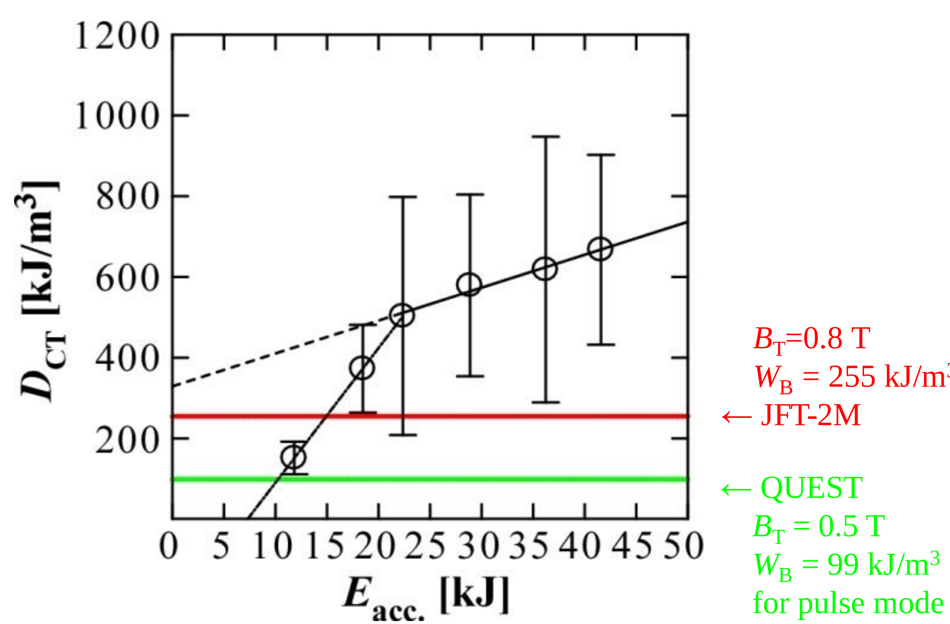

A CT plasma with high density (up to the order of 10^{21} m^{-3}) was injected perpendicularly from the outboard midplane along the major radius at a speed > 200 km/s.

CT Injection into OH ST Plasma

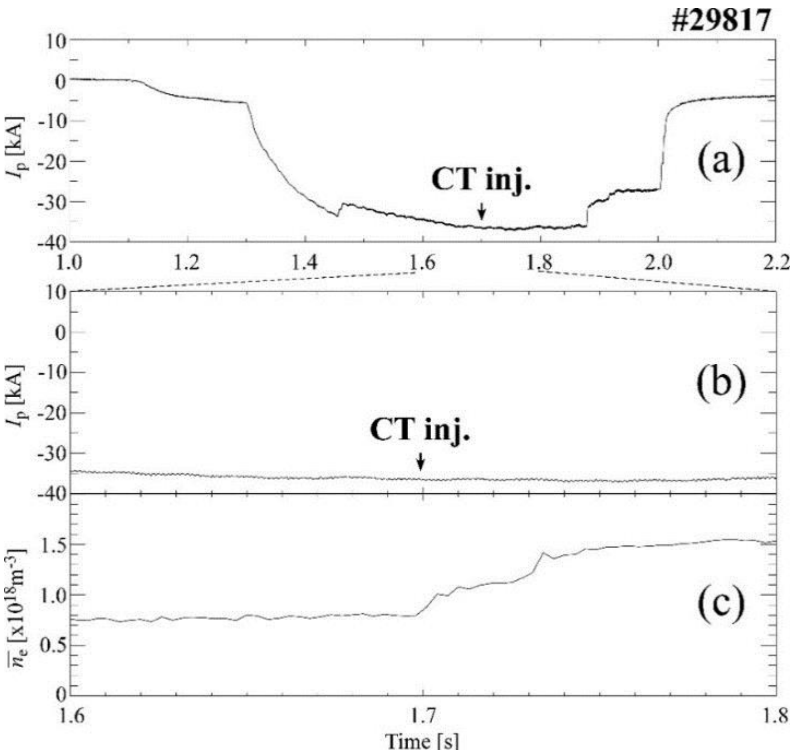

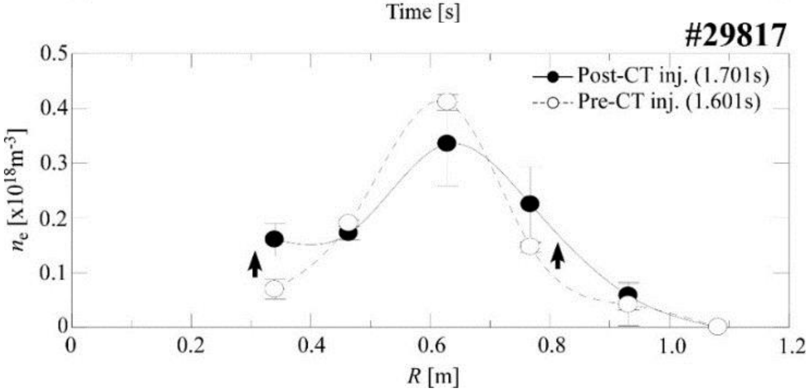

<u>CT plasma injection:</u>
($V_{CT\_form.}$= 17 kV and $V_{CT\_acc.}$= 25kV)

- ♦ CTI has no adverse effect on I_p.
- ♦ n_e increases just after CTI.

» Non-disruptive CTI was obtained.

<u>Thomson scattering measurement:</u>
♦ n_e is observed to increase on peripheral channels 0.5 ms after CTI.

Diffusion and equilibration times of CT injected particles in the vicinity of CT deposition:

- 50~100 μs for central CT deposition
- 1.4~2 ms for peripheral deposition

» Peripheral particle deposition by CTI was observed.

QUEST

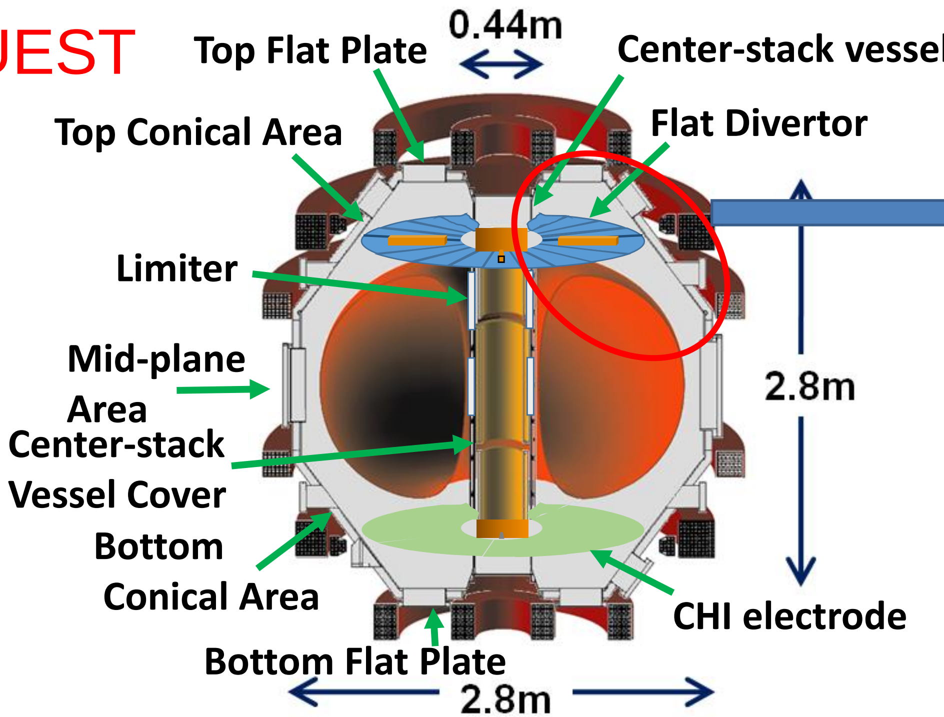

Hot wall was installed in 2014

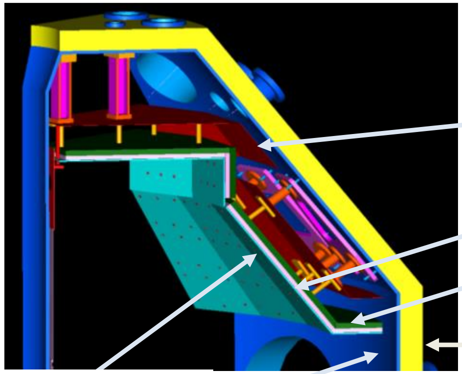

316L stainless steel coated with 0.1 mm thick APS-W, operated with T_{wall} = 393-523 K

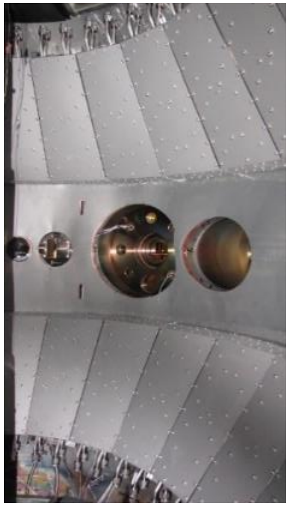

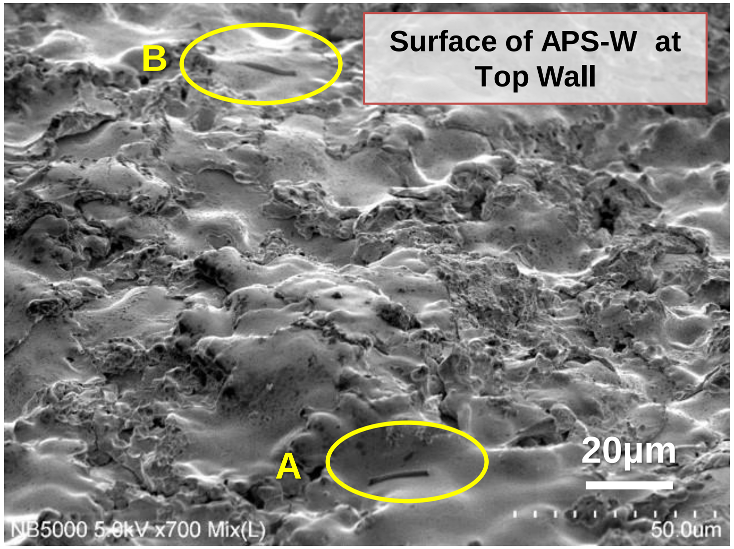

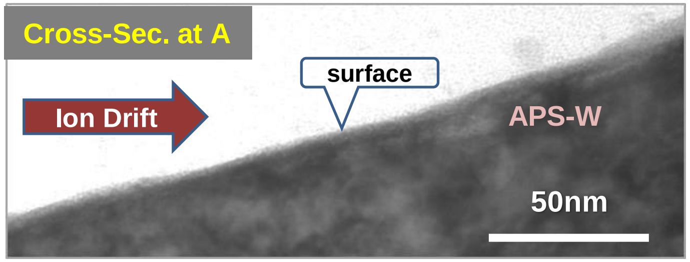

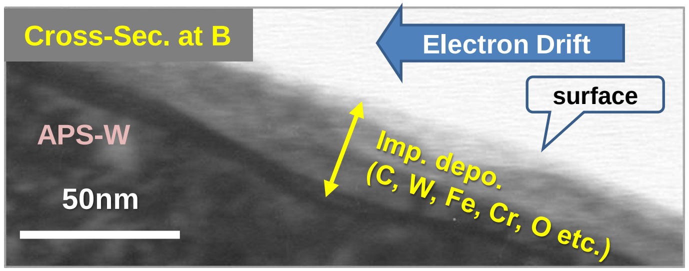

Progress Towards Steady State: 115 min Discharge Achieved with P_{RF} = 40 kW, T_{wall} = 393 K

Progress towards SSO (2010-2016)

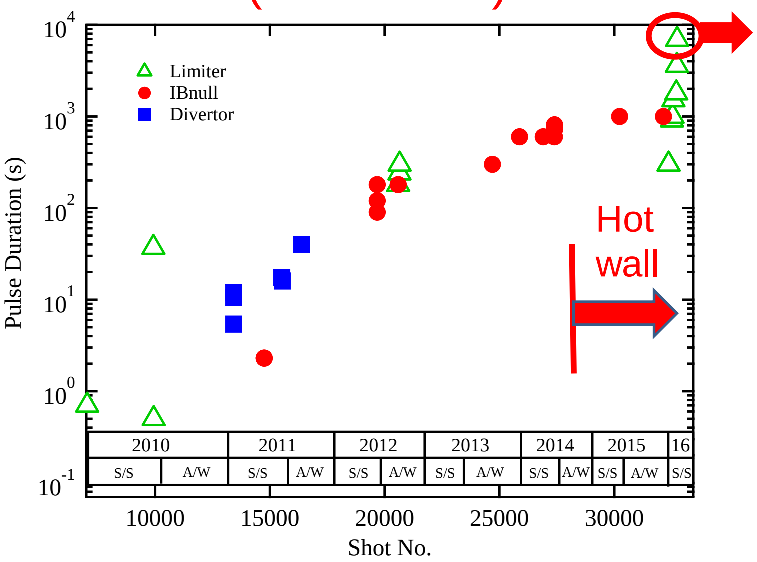

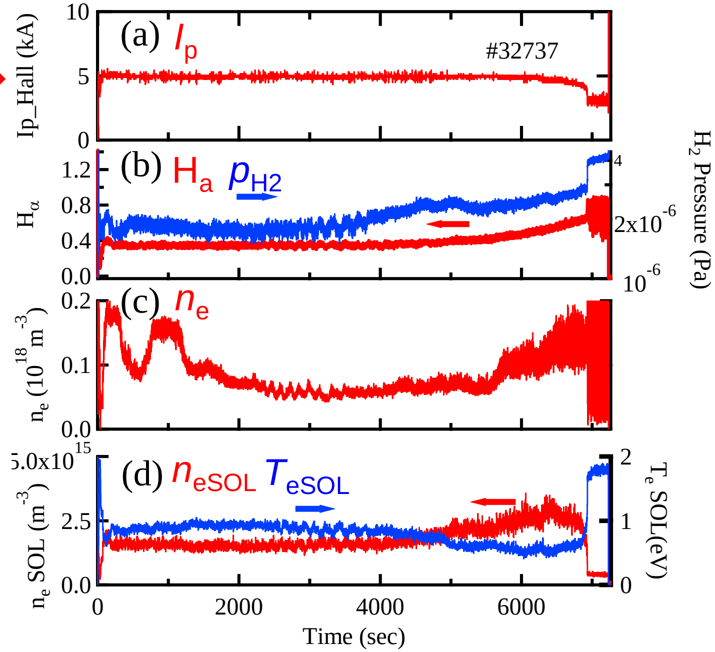

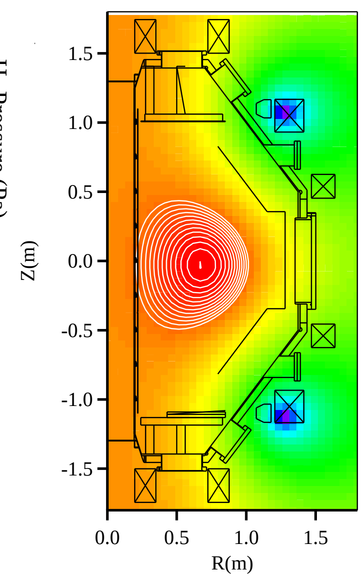

Microwave systems:

- 2.45 GHz : < 50kW
- 8.2 GHz: < 400kW
- 28 GHz: 300kW

Time Evolution of Wall Pumping Rate can be Reproduced by Hydrogen Barrier Model

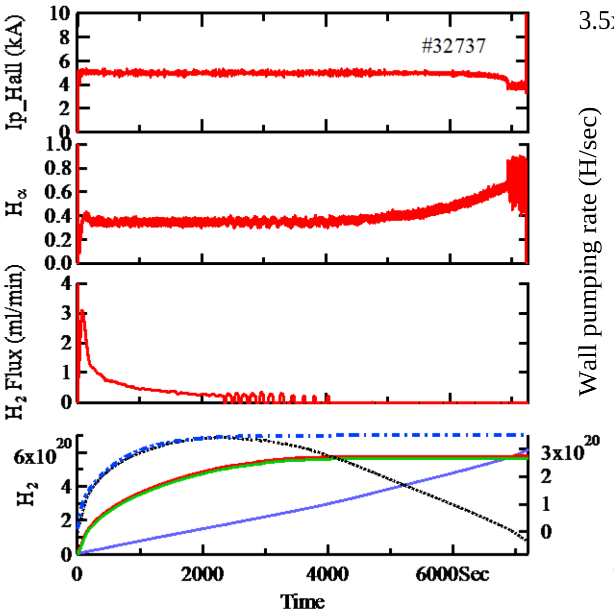

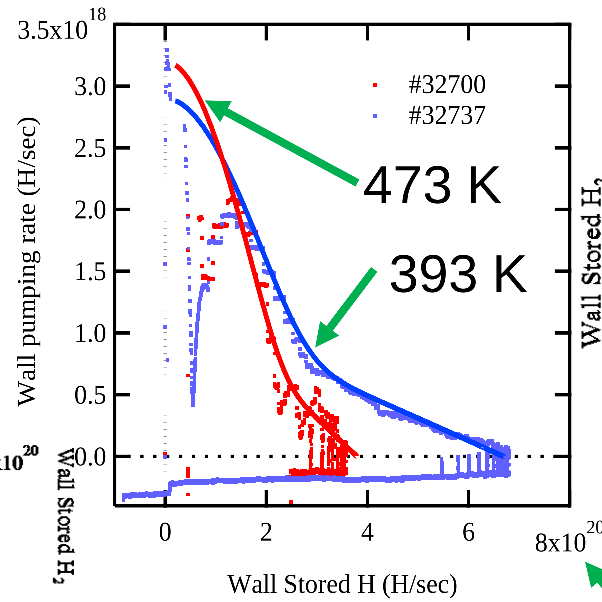

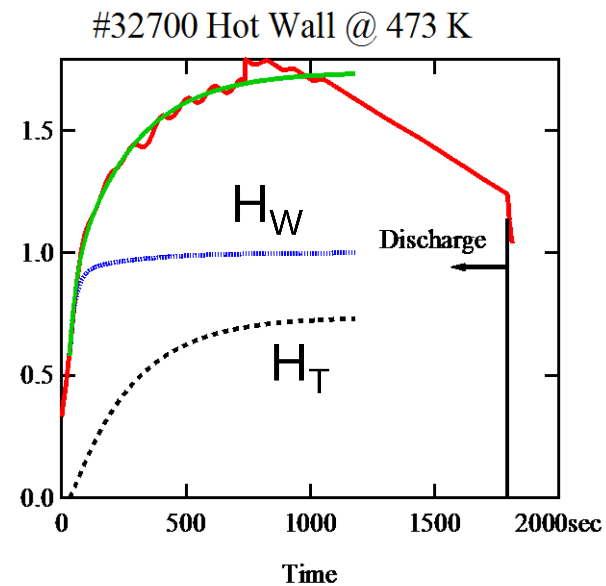

$$\frac{d(H_W+H_T)}{dt}=\Gamma_{in}S-\frac{k}{Sd_R^2}H_W^2$$

$$\frac{dH_T}{dt}=\alpha H_W\left(1-\frac{H_T}{H_T^0}\right)-\gamma H_T$$

dH_W/dt : wall pumping rate for H
H_W : number of H dissolved in wall
H_T : number of H trapped in defects
H_T^0 : upper-limit of H trapped in defects
S : surface area
G_{in} : net influx per unit of area into wall
k : surface recombination coefficient of H
d_R : thickness of deposition layer
a : H trapping rate
g : H de-trapping rate

#32737 (T_{wall} = 393 K: blue dots)
#32700 (T_{wall} = 473 K: red dots)
Solid lines indicate calculated results predicted by the hydrogen barrier model.

EX/P3-38 Y. Ono, et al.
PD/P-11 Inomoto, et al.

Merging/ Reconnection Heating for Direct Access to Fusion Reaction

A fusion reactor can maintain reaction, once D-T plasma with $n\tau > 10^{20}$ m^{-3} s is heated to > 10 keV.

The key is how to increase T_i to over 10keV.

In conventional tokamaks:
1st : Ohmic heating
$W = \eta I_t^2 \propto T_e^{-3/2} I_t^2$
+ 2nd : Additional heating
(NBI or RF)

Merging of two toroidal plasmas can increase their T_i .

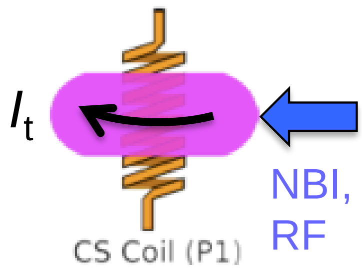

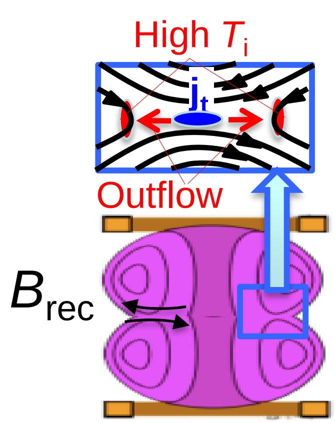

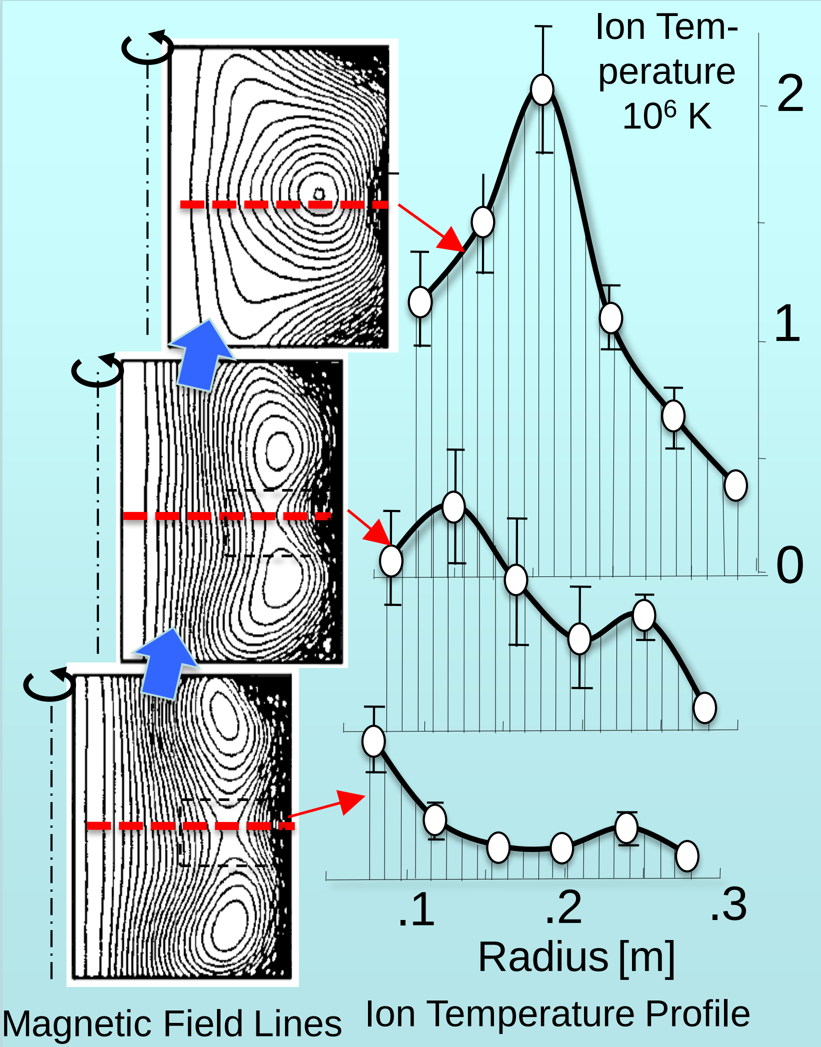

B_{rec}^2 Scaling of Reconnection Heating Indicates Direct Access to α-heating without NBI, Leading to New High-B_{rec} Experiments: ST-40 & TS-U

$$V_{outflow} \sim V_{pA} \propto B_p / n^{1/2}$$

$$\Delta W_{th} \sim \Delta W_{ion} \propto \Delta(nT_i) \propto \Delta T_i$$

(n ~ constant)

$$\propto B_{rec}^2 \propto B_p^2$$

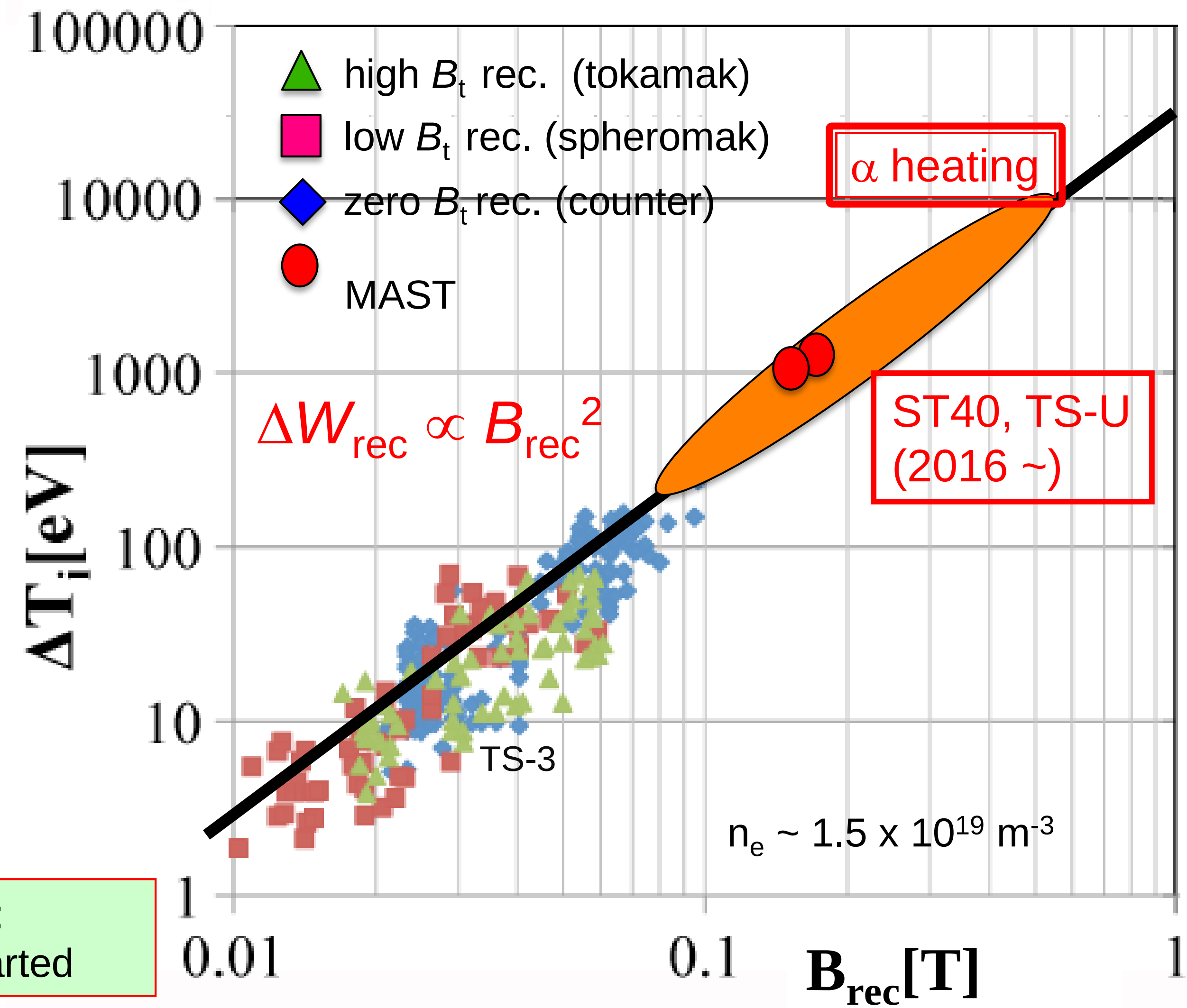

Construction of ST40 &TS-U:
high-B_{rec} merging devices started

ST40 : FIP/P7-19 M. Gryaznevich, et al.

T. Fujita, et al.
名古屋大学
NAGOYA UNIVERSITY

Stability Improvement by Helical Field

TOKASTAR-2
tokamak-helical hybrid device

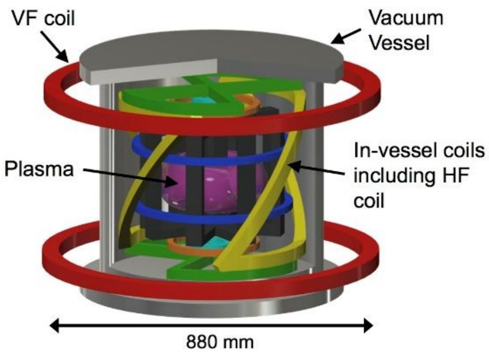

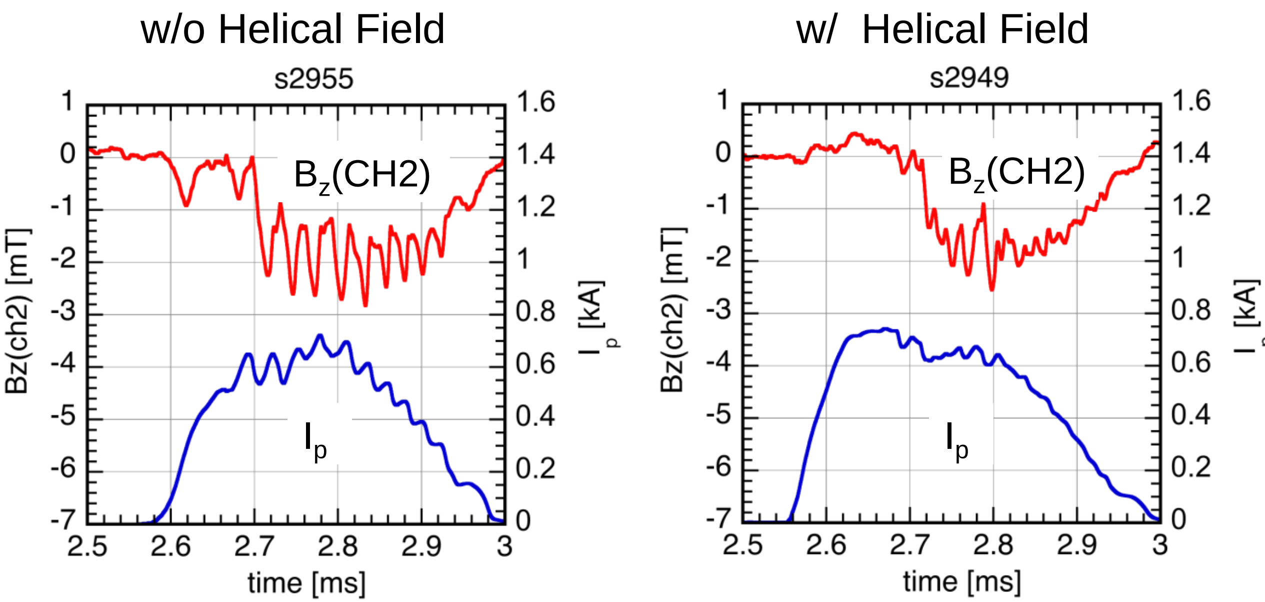

Tokamak discharges with and without helical field were compared.

Suppression of horizontal position oscillation by helical field application was observed by a magnetic probe inserted to the plasma core under a weak vertical field condition.

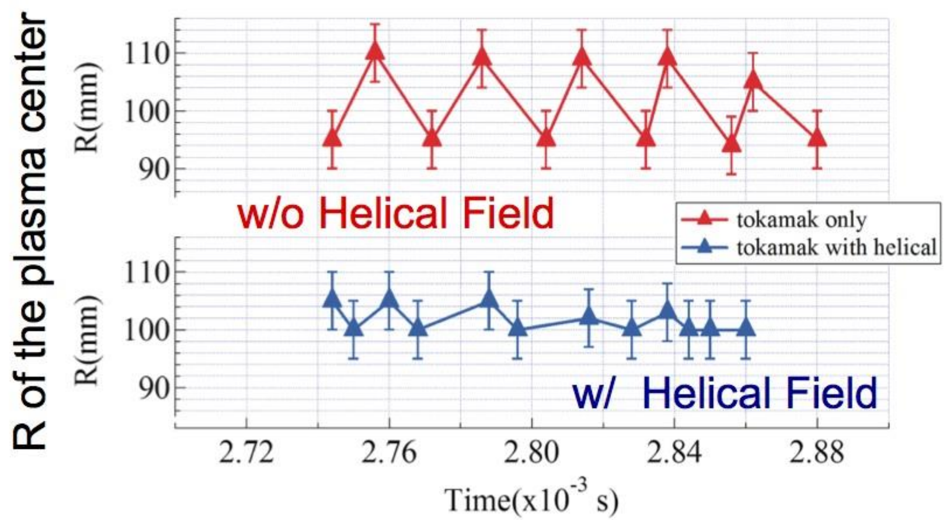

UEDA, T., et al., Plasma Fusion Res. **10** (2015) 3402065.

- The radial movement of tokamak plasma was studied without probe insertion by a high-speed camera.
- The plasma touched the outer wall repeatedly in a discharge without helical field. In a discharge with helical field, the plasma position was stable and touched the inner wall during the discharge.
- The stabilization effect of the external helical field on the tokamak plasma horizontal position was confirmed in the TOKASTAR-2 experiment.

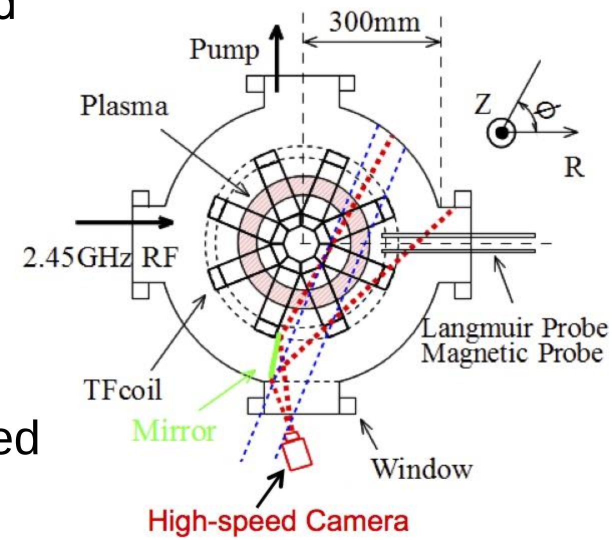

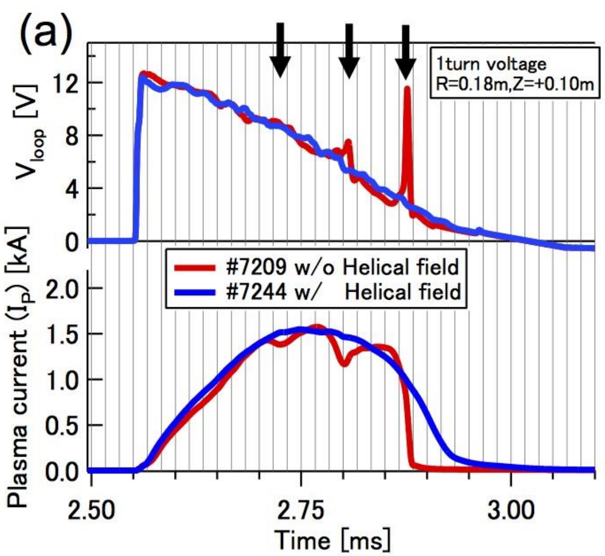

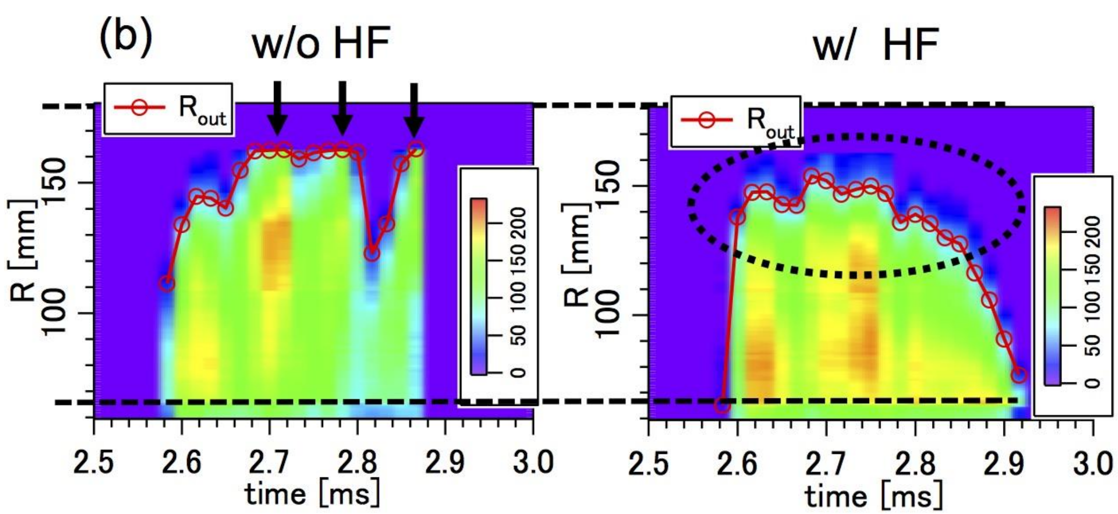

SAKITO, T., et al., Plasma Fusion Res. **11** (2016) 2402074.

For Further Details (at FEC2016)

- I_p Start-up
  - ECW/EBW (EX/P4-45 Tanaka, et al., EX/P4-50 Idei et. al.,)
  - LHW (EX/P4-48 Ejiri, et al.)
  - CHI (EX/P5-21 Nagata, et al.)
  - AC OH (EX/P4-48 Ejiri, et al.)
- Advanced Fueling
  - CT Injection (PD/P-16 Fukumoto, et al.)
- Steady-State Operation
  - Particle Control by High Temp. Wall (EX/P4-49 Hanada, et al.)
- Ultra-High-β Operation
  - Reconnection Heating (EX/P3-38 Y. Ono, et al., PD/P-11 Inomoto, et al.)